VOLUME 81 PAPER No. 842

PROCEEDINGS

AMERICAN SOCIETY
OF
CIVIL ENGINEERS

DECEMBER, 1955

THE ACTION OF SOFT CLAY ALONG FRICTION PILES

by H. B. Seed and L. C. Reese,
Associate Members, ASCE

SOIL MECHANICS AND FOUNDATIONS DIVISION

{Discussion open until April 1, 1956}

Copyright 1955 by the AMERICAN SOCIETY OF CIVIL ENGINEERS
Printed in the United States of America

Headquarters of the Society
33 W. 39th St.
New York 18, N. Y.

PRICE $0.50 PER COPY

THIS PAPER

--represents an effort by the Society to deliver technical data direct from the author to the reader with the greatest possible speed. To this end, it has had none of the usual editing required in more formal publication procedures.

Readers are invited to submit discussion applying to current papers. For this paper the final date on which a discussion should reach the Manager of Technical Publications appears on the front cover.

Those who are planning papers or discussions for "Proceedings" will expedite Division and Committee action measurably by first studying "Publication Procedure for Technical Papers" (Proceedings Paper No. 290). For free copies of this Paper—describing style, content, and format—address the Manager, Technical Publications, ASCE.

Reprints from this publication may be made on condition that the full title of paper, name of author, page reference, and date of publication by the Society are given.

The Society is not responsible for any statement made or opinion expressed in its publications.

This paper was published at 1745 S. State Street, Ann Arbor, Mich., by the American Society of Civil Engineers. Editorial and General Offices are at 33 West Thirty-ninth Street, New York 18, N. Y.

THE ACTION OF SOFT CLAY ALONG FRICTION PILES[a]

H. B. Seed[1] and L. C. Reese,[2] Associate Members, ASCE

Many piles derive a major part of their supporting capacity from skin friction. Dynamic formulas have proved to be of limited value for determining the bearing capacity of such piles, and static formulas appear to hold most promise for the development of rational design procedures. However, improvements in design methods are restricted by the limited available knowledge of the mechanics of the inter-action of piles and soil. This paper reports an investigation which attempts to further the understanding of the action of soil alongside friction piles.

Several 6-in. diameter pipe piles, 20 to 22 feet long, were driven about 15 feet into a stratum of soft, saturated clay. Electric strain gages were installed on one pile to measure load and pressure distribution along the pile. This pile was test loaded soon after driving and a number of times thereafter. Load distribution curves were obtained for several loads, including the ultimate load, for each test loading. Total pressures and pore-water pressures, caused by action of soil against the pile wall, were measured at several points along the pile length during the pile driving and during the load-test period.

Several borings were put down in the test area and undisturbed soil samples were obtained. Soil tests were made to establish the relationships between strength and water content for clay unaffected by pile driving, for clay next to a pile which had been in place 1 day, and for clay next to a pile which had been in place 30 days. The soil test results were interpreted to determine the effect of pile driving on the clay and the resistance of the clay to movement of the pile.

In addition a series of vane shear tests were made on the clay, and a procedure was developed for using the results of these tests to determine the load vs. settlement relationship for a pile driven into the clay. The load vs. settlement curve obtained in this way was compared with the results of load tests and suggestions made for the practical use of the procedure.

Location of Tests and Soil Conditions

The tests were conducted at a site adjacent to the San Francisco - Oakland Bay Bridge on the east side of San Francisco Bay. The soil conditions at this site (see Fig. 1) consisted of about 4 ft of fill, 5 ft of sandy clay, and then a layer of organic silty clay containing shells known locally as "bay mud," which extended to at least 30 ft below the ground surface. The ground water table was about 4 ft below the ground surface.

This site was chosen after extensive field tests had shown the soil conditions in the area to be relatively uniform.

---

a. A paper presented at the National Convention of the American Society of of Civil Engineers, February 7-11, 1955, San Diego, California.

1. Asst. Prof. of Civ. Eng., Univ. of California, Berkeley, Calif.
2. Prof. of Civ. Eng., Univ. of Texas, Austin, Tex.

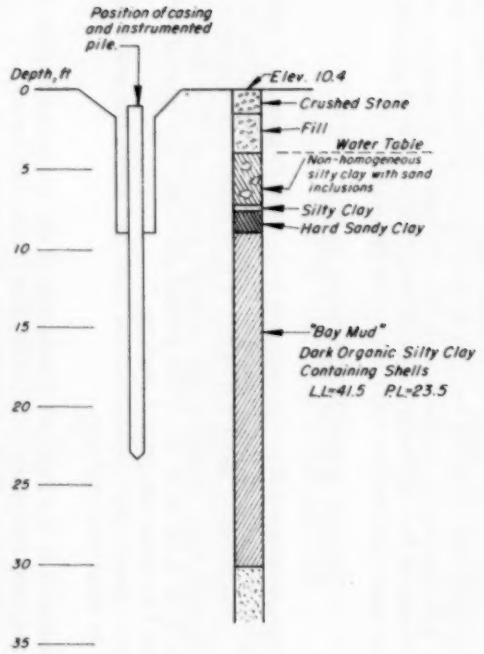

Fig. 1 SOIL PROFILE

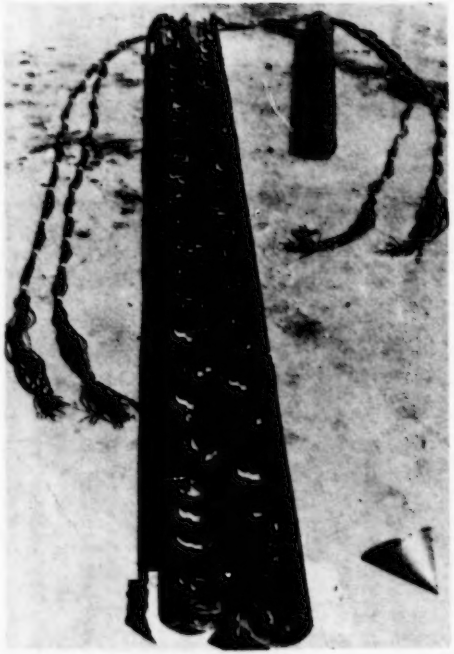

Fig. 2 VIEW OF INSTRUMENTATION

Fig. 3 PILE PRIOR TO DRIVING

Description of Piles

The piles used in the investigation were made from 6-in. diameter, spiral-welded steel pipe, No. 14 gauge, and were fitted with conical driving points. The pile to be instrumented was cut lengthwise along a diameter, so that the gages could be installed inside the pile.

The load-measuring gages were made by cementing SR-4 gages directly to the pile wall. The pressure gages will be described elsewhere. A view of the instrumentation, prior to the rejoining the pile halves by welding, is shown in Fig. 2, and the pile just prior to driving is shown in Fig. 3.

In order to eliminate the effects of the upper 9 ft of nonhomogeneous soil on the supporting capacity of the pile, a 12-in. diameter casing was installed to a depth of 9 ft, and the soil inside the casing was removed. The pile was then lowered to the surface of the clay at the bottom of the casing and driven into the clay using a 150-lb drop hammer. The soil profile and arrangement of the casing are shown in Fig. 1.

Several gages were damaged when the instrumented pile was driven, but a sufficient number of gages remained intact that data on load distribution and pressures against the pile wall were successfully obtained.

After the pile was driven to position, large changes were found to be taking place in the pressures at the pile wall. These pressures were read as rapidly as possible, and at the same time the loading apparatus was being prepared for the first load test. It was assumed that pile loading would affect the pressure measurements, but it was hoped that this effect would be small if the pile settlement was kept to a minimum. Readings during the preliminary load test and during several subsequent load tests indicated that loading caused little if any permanent effect on the pressure gage readings.

Results of Load Tests

The first load test was begun 3 hours after driving was completed; the second load test was begun 21 hours after driving was completed, and subsequent tests were run on the same pile at times suggested by the results obtained. These times were approximately 3, 7, 14, 23, and 33 days after driving was completed.

The pile was loaded in increments of 500 to 1000 lb for the first few loads, and the increments were decreased as the ultimate supporting capacity of the pile was approached. All of the load-measuring gages were read after the application of each load increment, except at loads near failure in several of the tests. The pressure gages were read usually after applying every second load increment.

Pile settlement during loading was measured by 2 dial gages, reading to 0.001 in. These dial gages were resting on opposite sides of the top of the pile, and their readings were averaged to obtain settlement. Load-settlement curves were plotted as the test progressed, and loading was stopped when settlement increased greatly with little increase in load.

The load-settlement curves for the seven load tests conducted are shown in Fig. 4. It was decided to consider the maximum load which the pile could support without continuous deformation during a loading as a measure of the bearing capacity of the pile at that time; therefore, since it was desired to keep settlements to a minimum, care was required in the application of load increments as the ultimate load was approached. Most of the curves indicate that loading was stopped as soon as the ultimate load was reached.

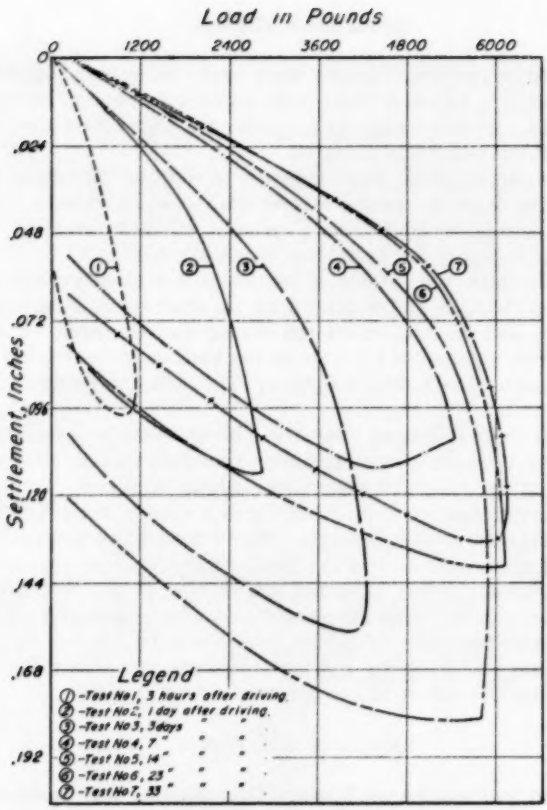

Fig. 4 LOAD *vs* SETTLEMENT CURVES.

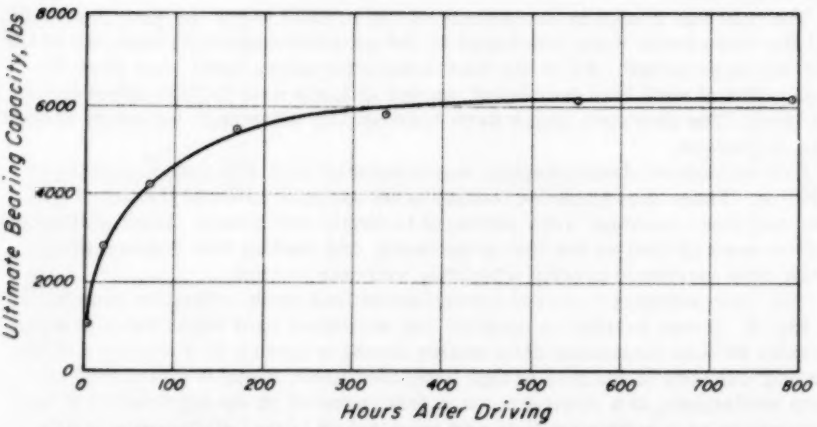

Fig. 5 INCREASE IN ULTIMATE BEARING CAPACITY WITH TIME.

For the first three loadings, as shown by Fig. 4, the settlement dials were read at zero load; in subsequent loadings it was found more convenient to take the first settlement reading after a small seating load had been applied, because of the difficulty in placing the settlement gages before the loading beam was positioned.

In practice, load tests are considered to be the best means of determining the supporting capacity of friction piles, and the load-settlement curves are interpreted in some way to determine the safe load which can be carried by the pile. The load-settlement curves obtained from these tests and many others which have been obtained for friction piles have a characteristic shape: an initial portion which is straight or slightly curved, a sharply curved transition portion, and a final portion which shows increasing settlement for no increase in load. The unloading curve is roughly parallel to the initial portion of the loading curve. The safe load is usually taken as some proportion of the ultimate load or as the load corresponding to some limiting value of settlement.

The loading procedure used in this project differs from that recommended by most authorities in that the time between load increments was quite short. Therefore, it can be expected that the shape of the load-settlement curves will differ from those which are usually obtained for a friction pile. Using the recommended procedure, there would have been a more gradual transition between the initial and final parts of the curve.

It was anticipated that there would be an increase in bearing capacity of the pile with time, but the magnitude of the increase, as shown in Fig. 5, was surprising. The ultimate load for the final test was 5.4 times as great as the ultimate load measured initially. The factor would have been greater had it been possible to determine the static bearing capacity of the pile immediately after driving instead of 4 hours after driving. About 88% of the increase in bearing capacity occurred in 8 days; the remaining 12% increase occurred during the next 25 days.

The change in strain-indicator reading for each load-measuring gage was multiplied by the appropriate calibration factor to obtain the load at each gage point. Measurements on opposite sides of the pile were averaged to obtain the load at each gage depth. A typical set of load distribution curves, as measured during a test, is shown in Fig. 6. The dotted curve which appears on the figure is an estimate of the load distribution which existed at the failure load. The load distribution could not be measured accurately at this stage because the pile was settling rapidly, and there was not time to obtain the gage readings while maintaining the low values of pile settlement desired. Fig. 7 shows the load distribution curves at the failure load in each of the load tests.

The mechanics of soil resistance to the downward movement of a friction pile is illustrated in Fig. 8. If the pile were completely rigid, all points of the pile would move downwards an equal amount and the soil deformation accompanying the downward movement of the pile would result in the development of shearing stresses in the soil resisting the downward movement. The shear stresses in the soil would cause the load in the pile to decrease with depth. Since piles are not completely rigid, the observed settlement of the top of the pile exceeds the downward movement of the pile tip by an amount equal to the elastic compression of the pile; and, since the shear resistance of the soil around the pile, which depends on the magnitude of the shear deformation, causes the load in the pile to decrease with depth, the actual movements of points on the pile wall will increase with their distances from the pile tip.

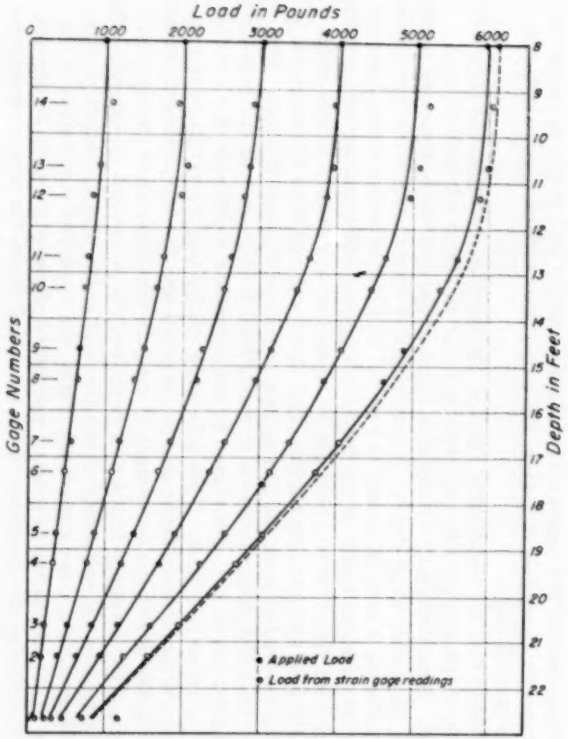

Fig. 6 LOAD DISTRIBUTIONS ALONG PILE FOR SEVENTH LOAD TEST.

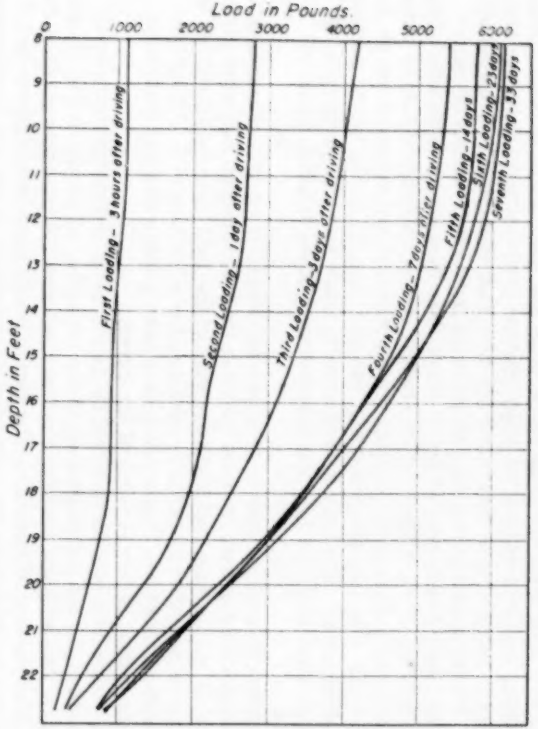

Fig. 7 LOAD DISTRIBUTION ALONG PILE AT FAILURE IN EACH OF THE LOAD TESTS.

It follows that the distribution of load along a friction pile is associated with the relative stiffnesses of the pile and the surrounding soil. Since the soil will invariably deform more readily than a pile, it is difficult to imagine a practical case in which there would be no load transmitted to the pile tip. It will be seen from Figs. 6 and 7 that in these tests about 90% of any applied load was transferred to the soil by shaft resistance and the remaining 10% was carried by the pile tip.

The load distribution curves in Figs. 6 and 7 show that very little load was removed by the top 3 ft of soil surrounding the pile. It is possible that this soil was displaced an extra amount by the vibration of the pile during driving and that the overburden pressure was insufficient to cause bond to develop; unfortunately not enough data was obtained from the pressure gages near the top of the pile to determine this possibility.

From a knowledge of the distribution of any applied load along a friction pile and the corresponding downward movement of the top of the pile, the following information may be obtained:

1. The rate of load transfer from pile to soil or the shearing resistance of the soil around the pile; at any point along the pile this is equal to the slope of the load distribution curve divided by the circumference of the pile.
2. The elastic compression of the pile from the top to any section along its length. This can be obtained by dividing the area under the load distribution curve to that section by the area of the pile and the modulus of elasticity of the pile material. The elastic compression can then be subtracted from the observed pile settlement to obtain the movement of the pile at the section under consideration.

Thus the shear resistance and the corresponding shear deformation of the soil around a pile at any point along the pile can be determined. The fact that such deformation can be obtained from load distribution curves suggests the possibility that shear resistance vs. deformation curves obtained from soil shear tests might be used to determine load distribution curves and load vs. settlement curves for friction piles; a procedure for determining such curves is presented later.

Results of Soil Tests

Laboratory Tests. The properties of the undisturbed soil were determined by a comprehensive series of tests on samples taken with a piston-type sampler in Shelby seamless steel tubes, 30 in. in length and 2.87 in. in diameter. Three borings, Nos. 1, 2, and 3 in Fig. 9, were put down in the vicinity of the field work, and samples were taken as nearly continuously as possible. Unconfined compression tests were performed on 23 samples and consolidation tests on 5 samples. In addition, 13 unconfined compression tests and 3 consolidation tests were performed on remolded samples of the soil.

The average of several determinations of the unit weight of the undisturbed silty clay was 112 lb per cu ft, and average values for the Atterberg limits were: Liquid Limit = 41.5, Plastic Limit = 23.5. The results of the unconfined compression tests on undisturbed and remolded samples are shown in Fig. 10; in these tests most of the undisturbed samples failed suddenly on reaching a strain of about 10 to 15%, and the sensitivity of the specimens was about 2. It was intended to trim the 2.87-in. diameter samples down to 1.4-in. diameter specimens for the unconfined compression tests but the presence of shells in almost all of the samples prevented trimming. It was difficult to

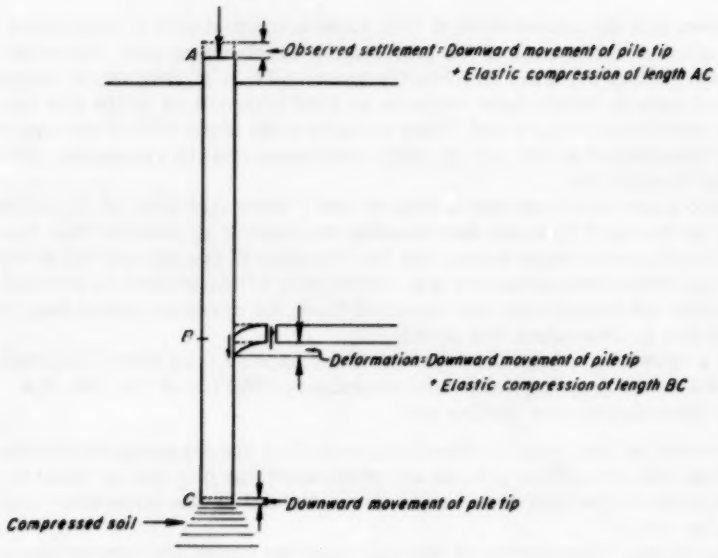

Fig. 8 MECHANICS OF SOIL RESISTANCE TO DOWNWARD MOVEMENT OF FRICTION PILE.

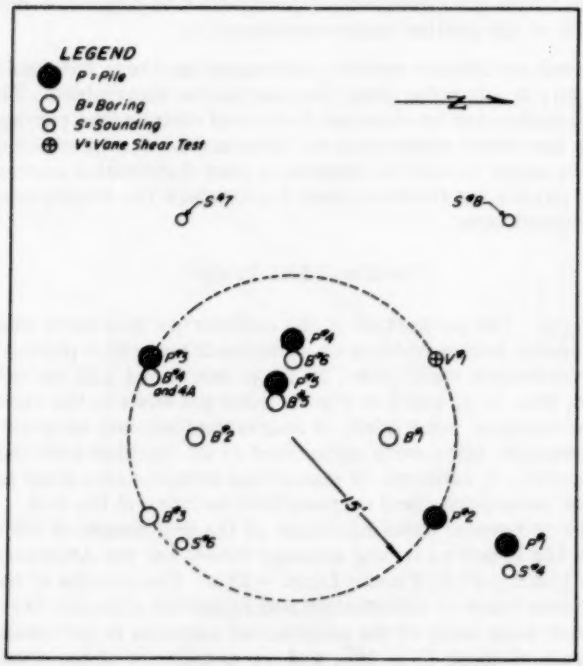

Fig. 9 LOCATION OF FIELD TESTS.

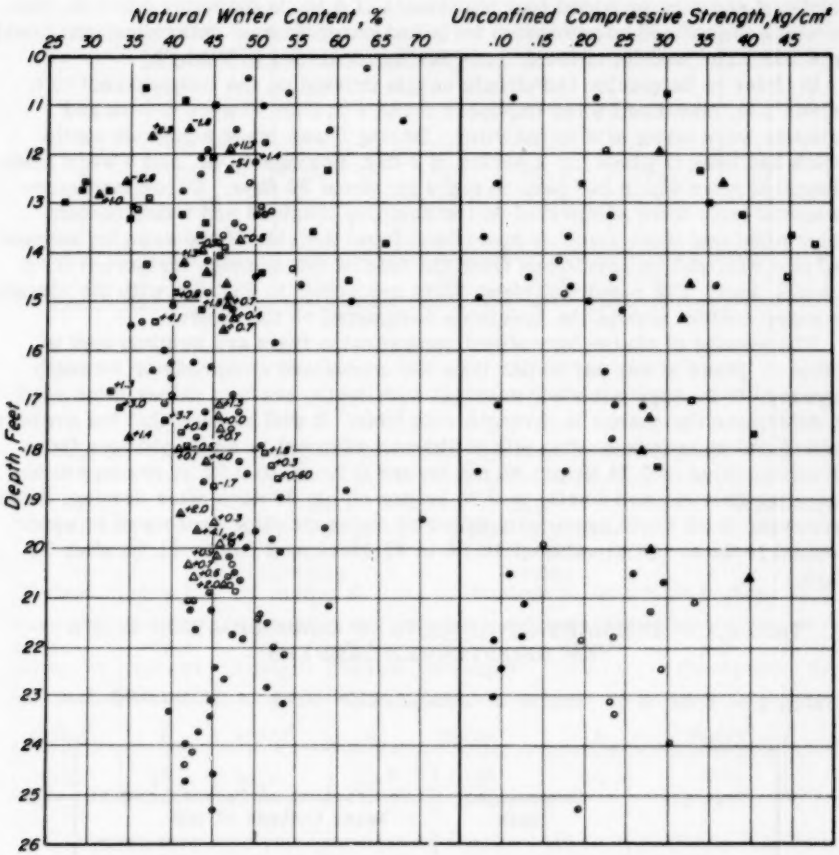

Legend:

- ● *Soil unaffected by driving, borings 1, 2, & 3.*
- • *Remolded soil.*
- △ *Soil next to pile 1 day after driving – boring 5.*
- ■ *Soil next to pile 30 days after driving – borings 4, 4A, & 6*

The number to the side of some of the points is to be added algebraically to obtain water content of part of sample farthest from pile.

Fig. 10 RESULTS OF SOIL TESTS.

find samples sufficiently free of shells for the preparation of consolidation test specimens. The results of the consolidation tests are summarized in Table 1, and typical results for both undisturbed and remolded soil are plotted in Fig. 11.

In addition to these tests, three large samples of remolded soil were reconsolidated under pressures of 1, 2, and 4 tons per sq ft. Each of the reconsolidated samples provided four specimens, 1.4 in. in diameter and 4 in. high, on which unconfined compression tests and water content determinations could be made. The results of these tests are summarized in Table 2.

In order to determine the effects of pile driving on the soil adjacent to a driven pile, additional piles (numbers 3 and 4 in Fig. 9) were driven and samples were taken next to the piles. Boring 5 was made alongside a pile which had been in place for a period of 1 day; Borings 4, 4A, and 6 were made alongside piles which had been in place for about 30 days. Unconfined compression tests were performed on the samples obtained and water content determinations were made on specimens from the side of the samples nearest the pile wall and on specimens from the side of the samples furtherest from the pile wall. The results of these tests are shown in Fig. 10, with the change in water content across the specimen designated on the figure.

The results of all the unconfined compression tests are summarized in Table 3. Since at any particular time the unconfined compression strength appeared to be approximately constant with depth, average values were used to determine the change in strength with time. It will be seen that the average unconfined compression strength of the soil adjacent to a pile changes from an initial value of 0.24 kg per sq cm before driving, to 0.32 kg per sq cm one day after driving, and finally to 0.36 kg per sq cm 30 days after driving; these increases in strength are accompanied by corresponding decreases in water content from an initial value of 48.1% to 43.6% after 1 day to 41.1% after 30 days.

TABLE 1 -- SUMMARY OF RESULTS OF CONSOLIDATION TESTS ON UNDISTURBED SAMPLES

TABLE 1 -- SUMMARY OF RESULTS OF CONSOLIDATION TESTS ON UNDISTURBED SAMPLES

Test No.	Compression Index	Coefficient of Permeability at Water Content of 40%
2-18LA*	0.36	1.7×10^{-8} cm/sec
2-18LB	0.40	2.9×10^{-8} cm/sec
3-25BA	0.45	2.1×10^{-8} cm/sec
3-25BB	0.45	2.3×10^{-8} cm/sec

* The first number represents the boring, the next 3 numbers represent the depth in inches to the sample.

TABLE 2 -- SUMMARY OF RESULTS OF UNCONFINED COMPRESSION TESTS ON RECONSOLIDATED SAMPLES

Test No.	Consolidation Pressure, tons per square foot					
	1		2		4	
	U.C. Strength	Water Content	U.C. Strength	Water Content	U.C. Strength	Water Content
	kg/cm^2	%	kg/cm^2	%	kg/cm^2	%
A	0.74	33.1	1.47	30.3	2.45	27.3
B	0.76	33.3	1.49	30.3	2.44	27.3
C	0.79	33.5	1.45	30.3	2.53	27.3
D	0.63	33.6	1.42	30.4	2.56	27.3
Avg.	0.73	33.4	1.46	30.3	2.49	27.3

TABLE 3 -- AVERAGE VALUES OF UNCONFINED COMPRESSION STRENGTH AND WATER CONTENT

Soil Unaffected by Driving Borings 1, 2 & 3		Soil Next to Pile-- 1 Day after Driving Boring 5		Soil Next to Pile-- 30 Days After Driving Borings 4, 4A & 6		Remolded Soil Borings 1, 2 & 3	
U.C. Strength	Water Content	U.C. Strength	Water Content	U.C. Strength	Water Content	U.C. Strength	Water Content
kg/cm^2	%	kg/cm^2	%	kg/cm^2	%	kg/cm^2	%
0.24	48.1	0.32	43.6	0.36	41.1	0.11	48.1

The percentage of shells, based on dry weight of solids excluding shells, in the unconfined compression tests specimens ranged from 0 to 17; the average percentage was about 7. Some of the shells were more than an inch wide. About 14% of the moisture samples were entirely free of shells. Disturbance of the soil due to sampling was probably greater for those samples which contained shells than for those relatively free from shells; however, examination of the data failed to indicate a decrease in unconfined compressive strength with an increase in shell content.

Field Tests. 'In situ' shear tests were made on the silty clay prior to pile driving using a vane shear device. The vanes were each 1.5 in. wide and 4.5 in. high and the rate of deformation was 10 degrees per minute. The results of these tests are shown in Fig. 13.

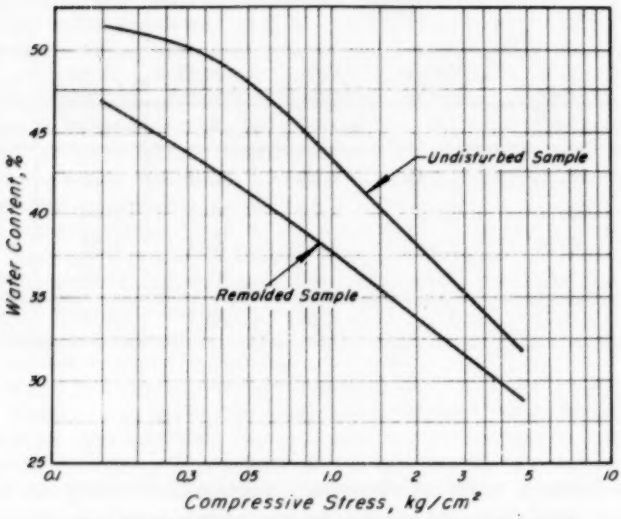

Fig. 11 CONSOLIDATION TEST DATA FOR UNDISTURBED AND REMOLDED SOIL.

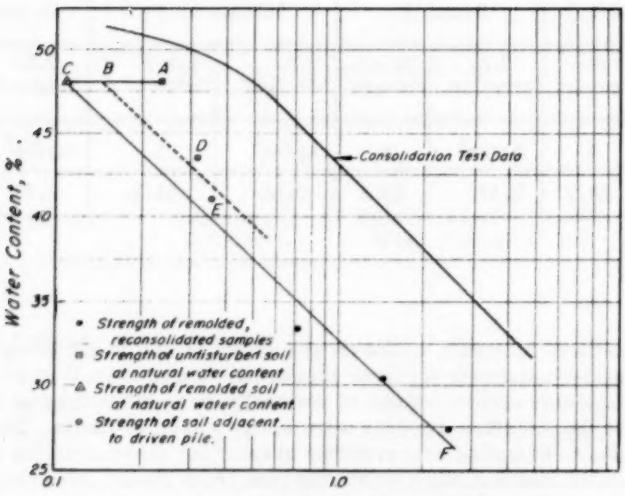

Fig. 12 STRESS AND STRENGTH *vs* WATER CONTENT RELATIONSHIPS.

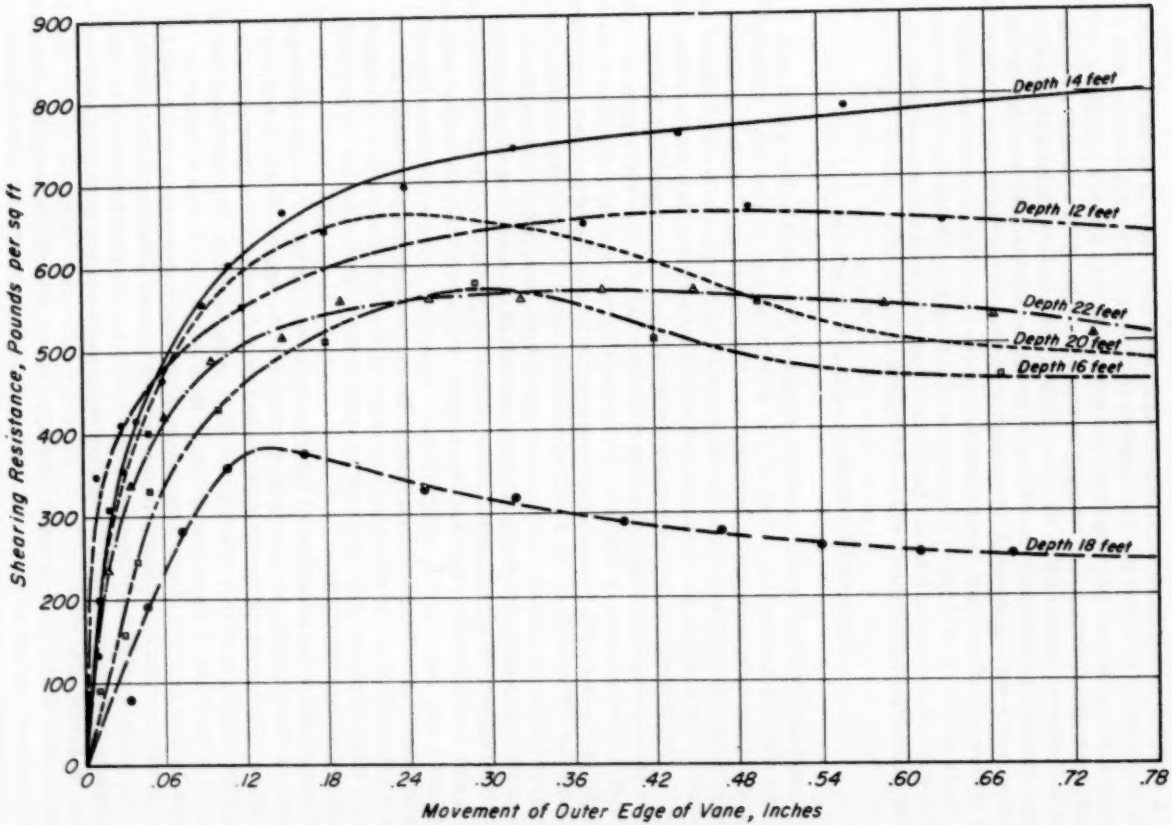

Fig.13 RESULTS OF VANE SHEAR TEST

The shear strengths determined by the vane tests were considerably higher than those indicated by the unconfined compression tests. This difference in strengths is probably due to the presence of shells in the soil, which appeared to have a marked effect on the vane shear strengths.

A 6-in. diameter hand auger was used to advance a hole to within about 2 ft of the depth at which the vane test was to be run. The vane device was then pushed or driven into position. In those instances where it could be pushed into position the shear strength was much lower than when the device had to be driven down. After the vane device had been withdrawn, the hand auger cuttings showed that the difficulty in advancing the vane was due to the presence of shells in the soil. Two series of vane shear tests were made and the stress vs deformation characteristics of the silty clay were determined at intervals of 2 ft of depth. The results shown in Fig. 13 are those exhibiting the lowest shear strength at any particular depth, and therefore are probably those least affected by the presence of shells.

Effect of Pile Driving on Soil Properties

Housel and Burkey[1] and Cummings, Kerkhoff, and Peck[2] have presented papers which discussed the effect of pile driving on soil properties. Rutledge[2] was able to show a reasonable quantitative interpretation of the data of Cummings, Kerkhoff and Peck based on the statement, "Previous work[3,4] has shown that on a semilogarithmic plot of test data for saturated natural clay, the compressive strength-water content relation is a curve parallel to the virgin (or essentially straight-line) part of the consolidation test curve."

Such a plot is shown in Fig. 12. The consolidation test data are those obtained from a test on an undisturbed sample, following the procedure suggested by Rutledge. Points A, C, D, and E were determined by soil tests as discussed above. Point A represents the average unconfined compression strength of undisturbed samples, and Point C shows the effect of remolding at no change in water content. Points D and E show results of unconfined compression tests and water content determinations on samples which had been taken next to piles installed 1 day and 1 month, respectively. Line C-F represents the compressive strength-water content relationship for reconsolidated remolded clay and was drawn from Point C through an average of 3 points determined by experiment. It will be seen that Line C-F is very nearly parallel to the virgin part of the consolidation test curve.

Point A shows the condition of the clay prior to pile driving. By drawing the dotted line parallel to Line C-F, through an average of Points D and E, Point B was obtained. It would appear therefore that Point B represents the condition of Clay next to a pile immediately after driving. The distance between Points A and B shows the strength loss of the soil due to remolding caused by pile driving. Excess hydrostatic pressure was set up in the soil by the pile driving and this pressure was related to consolidation of soil next to the pile. The dotted line represents the change in soil properties due to consolidation, with Points D and E showing the change occurring in 1 day and 1 month, respectively.

Other data which are pertinent here are those showing the variation in water content across samples taken near a pile. Examination of data in Fig. 10 shows that for samples represented by Point D, the water content was an average of 1.31% higher for those parts of the samples farthest away from the pile; and for samples represented by Point E the water content was 1.33% higher for those parts of the samples farthest away from the pile.

From the information which has been presented it can be argued with reason that the water content next to the pile wall is progressively decreased with the passage of time after the pile has been placed until some limit is reached, and that this decrease in water content is accompanied by an increase in the strength of the soil at the pile wall. The soil strength will be highest at the pile wall and it will decrease in some fashion with distance from the pile; therefore, Points D and E in Fig. 12 must represent an average value for soil properties near the pile, because the samples were taken over a 3-in. distance. One could speculate on the value of the unconfined compression strength at the pile wall on the basis of the difference in water content across the sample; however, when a friction pile is overloaded failure usually occurs in the soil at some distance away from the pile wall; hence, some average value of the shearing strength of the clay near the pile wall will correctly define the effective strength. It is interesting to compare the time-rate of increase in soil strength as determined by soil testing, with the time-rate of decrease in excess hydrostatic pressure as determined from pore-water pressure gages. Such a comparison is shown in Fig. 14 and there is excellent agreement between the rates.

Relationship Between Soil Properties and Load Test Data

From the results of a load test on a friction pile a value for the average skin friction may be computed by dividing the maximum load which the pile can support by the embedded area of the pile. However, the variation in skin friction with depth can be seen by examining the distribution of the failure load along the pile. The slope of this load distribution curve at any point is a measure of the rate of load transfer (skin friction) from the pile to the soil at that point. The rates of load transfer along the pile have been determined from the load distribution curves for the failure load in each of the load tests, and the results are shown in Fig. 15. In general the rate of load transfer at failure increases with increasing depth; it is about equal for depths of 20 and 22 ft., and it is very low for the shallow depths. The percentage increase in the rate of load transfer with time for all depths agrees in a general way with the percentage increase in bearing capacity of the pile.

In Fig. 15, the increase with time of the rate of load transfer from pile to soil (skin friction) at various depths in the soil when the pile is supporting its maximum load is compared with the increase in strength with time of the soil adjacent to the pile; the shear strength values used in this comparison were those on the dotted line closest to Points D and E in Fig. 12. For large values of time, there is good agreement between the shear strength of the soil and the rate of load transfer or skin friction at the greatest depths; for small values of time the agreement is not so good, with the skin friction being appreciably less than the shear strength of the soil. The bearing capacity of the pile, computed on the assumption that the full shear strength of the soil is developed over the embedded area of the pile, would be greater than the measured value with the largest error occurring at small times. A similar lack of agreement between bearing capacity and strength data is shown in Fig. 14 where it may be seen that in the early stages after driving, the time-rate of increase in shear strength is considerably greater than the time-rate of increase in bearing capacity. In making the above comparisons it is assumed that the shear strength of the soil is constant along the length of the pile since the test data in Fig. 10 show no definite trend in the shear strength vs. depth relationship.

At the outset of this investigation it was assumed that the failure which occurs when a friction pile is overloaded occurs in the soil surrounding the pile and not at the interface between pile and soil. However, the above results

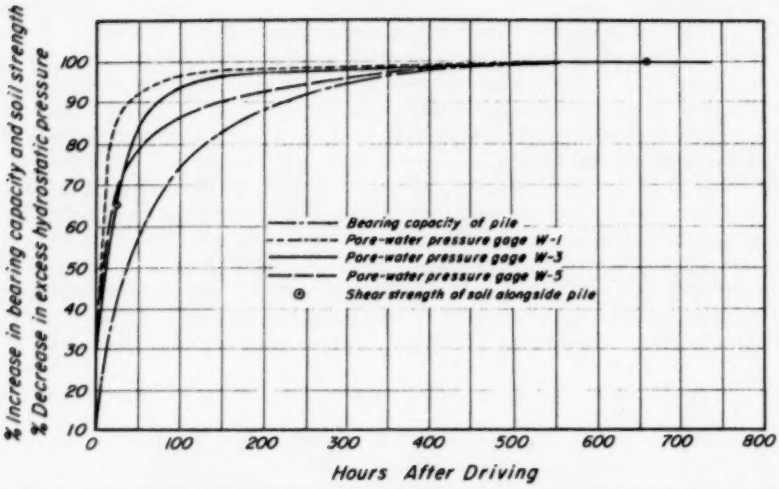

Fig. 14 COMPARISON OF RATE OF CHANGE OF BEARING CAPACITY, SOIL STRENGTH AND EXCESS HYDROSTATIC PRESSURE.

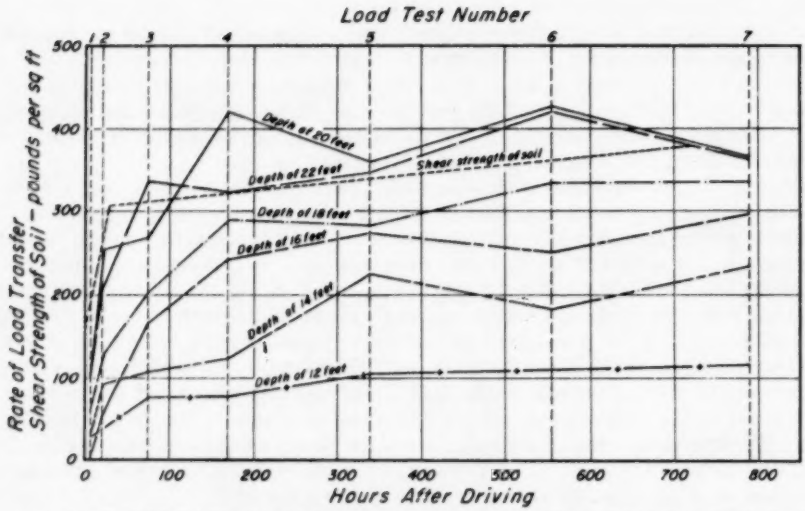

Fig. 15 INCREASE IN RATE OF LOAD TRANSFER FROM PILE TO SOIL AT VARIOUS DEPTHS COMPARED WITH INCREASE IN SHEAR STRENGTH OF SOIL NEXT TO PILE.

indicate that for the pile used in this investigation this assumption should be modified as follows: for small values of time for all depths, and for all values of time for the shallow depths, the failure which occurred when the pile was overloaded did not occur in the soil but at the interface between soil and pile.

Arguments which favor this modified hypothesis are:

1) The bearing capacity at time zero, as determined by extrapolating the bearing capacity vs. time curve in Fig. 5, was about 700 lb. The shear strength of the remolded clay, as determined by one half the unconfined compression strength of remolded samples, was 110 lb per sq ft; if this shear strength were effective over the entire embedded area, the bearing capacity of the pile at time zero would have been 2,360 lb. That the bearing capacity was less than one-third of the value indicated by the remolded shear strength probably indicates that failure occurred at the interface between pile and soil where a lower shearing resistance was developed.

2) The unconfined compression tests showed no significant variation of the soil strength with depth, either before or after pile driving; but Fig. 15 shows significant changes in the rate of load transfer with depth. The changes in the rate of load transfer probably indicate that bond failed to develop at the interface between pile and soil at the shallow depths.

3) The data in Fig. 14 showed good correlation between excess hydrostatic pressures and shear strength, but the increase in bearing capacity lags behind for small values of time. The lower rate of increase in bearing capacity probably indicates a lag in the development of bond at the interface.

It is recognized that the modified assumption derives only from experiences with the piles used in this research; however, it seems probable that the modification will apply to other piles as well.

It is interesting to note that near the top of the pile, the maximum skin friction was less than the shear strength of the undisturbed soil due to the fact that failure occurred at the interface between pile and soil, while near the bottom of the pile, the maximum skin friction was greater than the shear strength of the undisturbed soil due to the increase in strength of the soil caused by disturbance and reconsolidation. It might be expected therefore that the average skin friction at failure, after sufficient time had elapsed to allow the soil around the pile to fully reconsolidate, would have a value approximately equal to the shear strength of the undisturbed soil. That this is in fact the case may be readily seen if the supporting capacity of the pile is computed on the assumption that the skin friction over the embedded area of the pile is equal to the shear strength of the undisturbed soil. The total skin friction, based on this assumption, is 5,400 lb., which together with a resistance of about 200 lb. at the pile tip, gives a total supporting capacity of 5,600 lb. This compares favorably with the maximum supporting capacity of 6,100 lb. measured in the seventh load test. It appears that this method of computing the ultimate supporting capacity of the test pile gives good results because the length of the pile was such that the error due to over-estimating of the skin friction at the upper end of the pile is approximately neutralized by the error due to under-estimation of the skin friction at the lower end of the pile.

Determination of Load Distribution and Settlement for A Friction Pile from Soil Shear Tests

In the discussion of the load distribution curves, the possibility of using data from shear tests of soil to obtain load distribution curves and load vs. settlement curves for a pile was mentioned. The accuracy of the results

obtained will depend, of course, on the validity of the soil test data; if, however, reliable data on the shear characteristics of the soil adjacent to the pile can be determined, the behavior of the pile under load can be predicted by the following method of analysis.

If a friction pile is driven through clay, the clay is remolded; consequently, regardless of the properties of the undisturbed soil, the clay in the vicinity of the pile has nonbrittle stress-deformation characteristics. A loaded pile produces deformation in the surrounding soil, and the deformation varies from a maximum at the ground surface to a minimum at the pile tip. In usual cases, the pile is quite stiff compared to the soil, so that at the ultimate pile load even the bottom-most soil elements will develop their maximum shear resistance. Although the top-most soil elements will be deformed more because of the elastic compression in the pile, the additional deformation will not cause this shear resistance to be reduced below the maximum values. Thus, the load distribution at the ultimate pile load can be determined from a knowledge of the shear strength of the soil around the pile. It is possible that there will be failure at the interface between pile and soil; if so, some fraction of the shear strength of the soil might be used to account for the loss of strength due to the interface failure.

For a number of reasons it is useful to know the load distribution along a friction pile which is supporting a load less than the ultimate. In this case three difficulties present themselves: how to compute the resistance of the pile point, how to relate stress-deformation curves for the soil to pile movement, and how to make the mathematical solution. At the present time the first two problems can be resolved approximately while the mathematical solution can be made by a method of successive approximations.

The resistance of the pile point in clay for a given downward movement of the pile point may be of minor importance if the pile support is supplied principally by shaft resistance: but for a complete solution the point resistance must be considered. Ultimately it is hoped that a method for determining point resistance based on the stress vs. strain characteristics of the soil determined from triaxial compression tests, can be developed. However as a temporary expedient, where the point resistance is very low, the resistance may be computed, as in the example which follows, by considering the point to be replaced by an equivalent length of shaft. The amount of shaft area to be added might be obtained by theoretical considerations or, as in the example, from the results of tests.

A more difficult problem is to relate the stress-deformation curves of the soil to the movement of the pile. If a point on the pile is assumed to move downward a certain amount, this downward movement must be related to the shear deformation in the soil at that point in order to determine a corresponding shear stress which will develop a resisting force along the pile. The methods of elasticity are of limited assistance in this problem since the soil is non-elastic. The stress vs. deformation curves used in this analysis should be those of the reconsolidated soil adjacent to the pile. However, such data cannot be readily determined and therefore, as a trial, it is suggested that the stress-strain curves obtained from vane shear tests on the undisturbed soil be applied. The vane imposes deformations similar to those imposed by a downward-moving pile and the radial movement of a point on the vane extremity is assumed to develop the same shear resistance as will an equal downward movement of a point on the pile. An attempt can be made to correct for the fact that failure may occur at the interface between pile and soil rather than in the soil by using only a certain proportion of the soil strength corresponding to a particular deformation.

The differential equation which defines the load distribution along the pile length can be approximated by considering an element cut perpendicular to the pile axis,[5] as shown in Fig. 16. The movement of the pile wall at depth z differs from that at depth z + dz by the elastic compression of the length dz of the pile. The unit strain of the pile at depth z is therefore:

$$\frac{d\phi}{dz} = \frac{P}{EA}$$

where E = modulus of elasticity of pile material
ϕ = movement of pile at depth z
P = load on pile at depth z

Then $$P = EA\frac{d\phi}{dz}$$

and $$\frac{dP}{dz} = EA\frac{d^2\phi}{dz^2} \quad \ldots\ldots\ldots\ldots\ldots\ldots\ldots\ldots\ldots\ldots (1)$$

Now if β is a function which defines the properties of the soil such that $\beta\phi$ is the shear resistance of the soil corresponding to a strain ϕ, then

$$dP = \beta\phi C dz$$

and $$\frac{dP}{dz} = \beta\phi C \quad \ldots\ldots\ldots\ldots\ldots\ldots\ldots\ldots\ldots\ldots (2)$$

Equating expressions in (1) and (2)

$$EA\frac{d^2\phi}{dz^2} = \beta\phi C$$

and $$\frac{d^2\phi}{dz^2} - \propto \beta\phi = 0 \quad \ldots\ldots\ldots\ldots\ldots\ldots\ldots\ldots\ldots\ldots (3)$$

where $$\propto = \frac{C}{EA}$$

This analysis ignores any deformation of a soil element next to the pile wall due to the non-uniform distribution of vertical load in the soil above this element and to this extent is approximate. The term β will be a constant only if there is a linear relationship between soil resistance and pile movement, as expressed by a line such as 1 in Fig. 17, for the full length of the pile. In that case and if $\propto$ is also constant, a theoretical solution can readily be obtained for the differential equation. A theoretical solution can probably be obtained conveniently if the soil resistance and pile movement are related by a curve such as 2 in Fig. 17 for the full length of the pile. However, the usual case is that the soil resistance and pile movement are related by such a curve as 3 in Fig. 17 and that this relationship will vary with depth. In this case, a numerical procedure seems most suitable for the solution of the differential equation, Equation (3). The procedure is analogous to the test loading of a pile, resulting in a series of load-distribution curves and in a load-settlement curve.

Computations Using Theory

In order to illustrate the proposed method of analysis, computations have been made to determine the load distribution curves and load vs. settlement relationship for the pile tested in the field. The stress vs. deformation

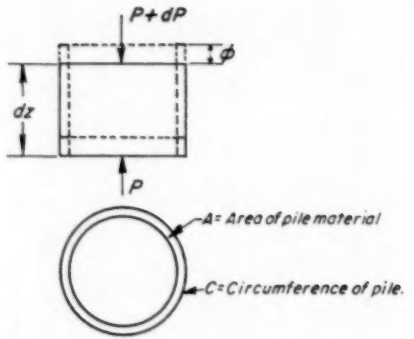

Fig. 16 ELEMENT FROM LOADED PILE.

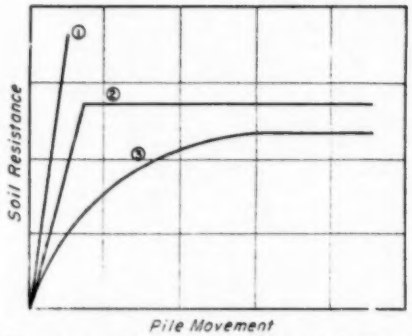

Fig 17 PILE MOVEMENT VERSUS SOIL RESISTANCE CURVES.

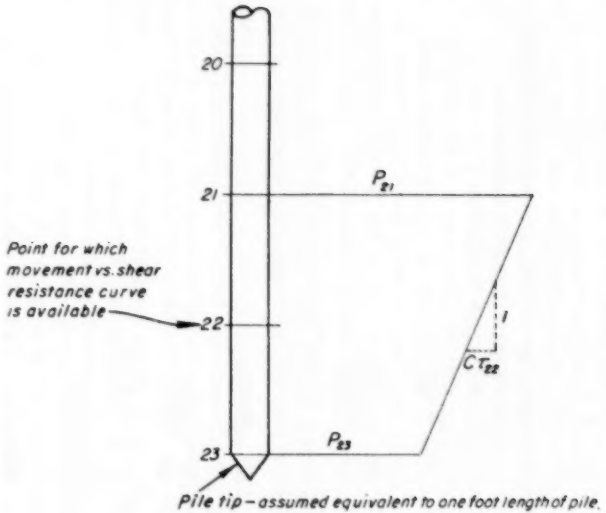

Fig.18 PORTION OF COMPUTED LOAD DISTRIBUTION CURVE.

relationships for the undisturbed soil determined by vane shear tests, shown in Fig. 13, were used in the analysis.

In order to correct for the fact that failure was found to occur at the interface between pile and soil rather than in the soil, only a certain proportion of the soil strength, corresponding to a particular deformation, was used. The proportions for the various depths were obtained from an examination of Fig. 15. A comparison of the shear strength of the soil with the rate of load transfer at the various depths enabled the following proportions to be obtained: 22 ft, 1.0; 20 ft, 1.0; 18 ft, 0.9; 16 ft, 0.7; 14 ft, 0.6; 12 ft, 0.3; 10 ft, 0. It is recognized that such factors, to be applied at various depths, would not normally be known. However, experience with other piles and soils may ultimately be used to select appropriate factors.

A particular load distribution curve is computed by assuming first a small downward movement of the pile tip. The stress-deformation curve for the soil at that depth is consulted, see Fig. 13, and the rate of load transfer which is developed is obtained. The load on the pile tip is obtained by multiplying this rate of load transfer by the shaft area which is assumed to replace the pile tip. In this case it was found that the resistance of the pile tip could be approximated by the shaft resistance on an additional 8 inches of pile length.

Next, a somewhat greater downward movement is assumed for a point on the pile a short distance higher, and for which a corresponding stress-deformation curve for the soil is available. The rate of load transfer for the assumed movement is obtained, and the increase of load in the pile can be computed. Then, using the area and modulus of elasticity of the pile material, the movement corresponding to this increase in load can be calculated. If the calculated movement does not agree with the assumed movement, a new computation is made and the process is continued until agreement between movements is obtained. In this manner, a load distribution curve can be computed for the entire pile length, corresponding to any assumed movement of the pile tip.

For the computation shown in Table 4 the downward movement of the pile tip at a depth of 23 ft was assumed to be 0.12 in. The stress vs. deformation curve for the soil at a depth of 22 ft was consulted and a rate of load transfer of 510 lb per sq ft was obtained. The area of shaft for 8 in. of pile length was 1.05 sq ft; therefore the load on the pile point was computed as 535 lb.

The movement, ϕ, of the pile for a depth of 22 ft was assumed to be 0.1210 in. Then the rate of load transfer of 510 lb per sq ft was obtained from the appropriate stress vs. deformation curve in Fig. 13.

The load in the pile at a depth of 21 ft was computed as follows (see Fig. 18)

$$P_{21} = P_{23} + \tau_{22} \cdot C \cdot L_{23\text{-}21}$$

where P_{21} = load in pile at a depth of 21 ft

P_{23} = load in pile at a depth of 23 ft

τ_{22} = rate of load transfer per unit area at a depth of 22 ft

C = circumference of pile

$L_{23\text{-}21}$ = length of pile from 23 to 21 ft

Thus

$$P_{21} = 535 + (510)\,(1.57)\,(2)$$

$$= 2125 \text{ lb.}$$

TABLE 4 — COMPUTATION OF THE LOAD DISTRIBUTION ALONG A FRICTION PILE FOR AN ASSUMED POINT MOVEMENT OF 0.0012 INCHES

Section Depth	Assumed Mid-point Movement	Load Transfer Developed	Surface Area	Load Increment	Total Load	Average Load	Compression of Section	Total Movement	Mid-point Movement
ft	in.	lb/ft^2	ft^2	lb	lb	lb	in.	in.	in.
	.1200	510	1.05	535				.1200	
23-21	.1210	510	3.14	1590	2125	1330	.0008	.1208	.1204
	.1204	510	3.14	1590	2125	1330	.0008	.1208	.1204
21-19	.1217	600	3.14	1880	4005	3065	.0018	.1226	.1217
19-17	.1239	340	3.14	1070	5075	4540	.0026	.1252	.1239
17-15	.1268	328	3.14	1030	6105	5590	.0032	.1284	.1268
15-13	.1303	380	3.14	1190	7295	6700	.0038	.1322	.1303
13-11	.1343	170	3.14	535	7830	7565	.0043	.1365	.1343
11-1					7830		.0224	.1589	

To check the assumed movement of the pile, $\phi = 0.1210$ in., at a depth of 22 ft. the movement of the pile at a depth of 21 ft was computed as follows:

$$\phi_{21} = \phi_{23} + \frac{P_{23} + P_{21}}{2} \frac{L_{23-21}}{AE}$$

where ϕ_{21} = movement of the pile at a depth of 21 ft

A = cross-sectional area of pile material (1.4 in^2)

E = modulus of elasticity of pile material (30 x 10^6 psi)

Thus $$\phi_{21} = 0.1200 + \frac{535 + 2125.}{2} \frac{24}{(1.4) \times (30 \times 10^6)}$$

$$= 0.1200 + 0.0008 = 0.1208$$

The movement of the pile at a depth of 22 ft was assumed to be the average of the movements at 23 and 21 ft, that is 0.1204 in. It is obvious that a more accurate calculation could be made by using the area under the load distribution curve from 23 to 22 ft, but the extra work involved does not appear to be justified. Thus, the computed movement at a depth of 22 ft of 0.1204 in. is not in agreement with the assumed movement of 0.1210 in. A new assumption was made and the calculation was repeated, as shown in Table 4, until agreement was obtained between assumed and calculated movements. Table 4 shows the entire computation for the full length of the pile.

By assuming various movements of the pile point, a series of load distribution curves can be obtained. The series obtained for this pile is shown in Fig. 19. For each assumed point movement, corresponding values for movement and load at the top of the pile are determined. Reference to Table 4 shows that for the assumed point movement of 0.120 in., the movement of the top of the pile is 0.159 in. and the load at the top of the pile is 7830 lb.

Movements and loads for the top of the pile can be plotted to obtain a load-settlement curve, as shown in Fig. 20.

Comparison of Theoretical and Test Results

In Fig. 19 the load distribution curves computed as described above are compared with the actual load distribution curve for the maximum load the pile was able to support (the ultimate load in the seventh load test). In Fig. 20 the computed load-settlement curve is compared with the load-settlement curve for the seventh load test. The results do not compare very favorably. However, the lack of agreement in this case is believed to be due to errors associated with the use of the vane shear device for determining the properties of the particular soil used in this investigation. The presence of shells in the soil, cutting across the failure plane, undoubtedly caused an increase in the resistance to movement of the vane with the result that the resistances computed from the dimensions of the vane were too high. This is evidenced by the fact that the shear strengths determined from the vane tests were higher than the maximum values of the rate of load transfer measured on the test pile. In a more uniform soil for which a vane test would give more reliable results, the method of analysis would probably give better agreement between computed and actual pile performance.

Even with a soil such as that used for this investigation, however, the proposed method may have useful practical applications. If vane shear tests are performed at a site where a friction pile is being test loaded, a pair of curves such as those shown in Fig. 20 could be obtained. From a practical standpoint,

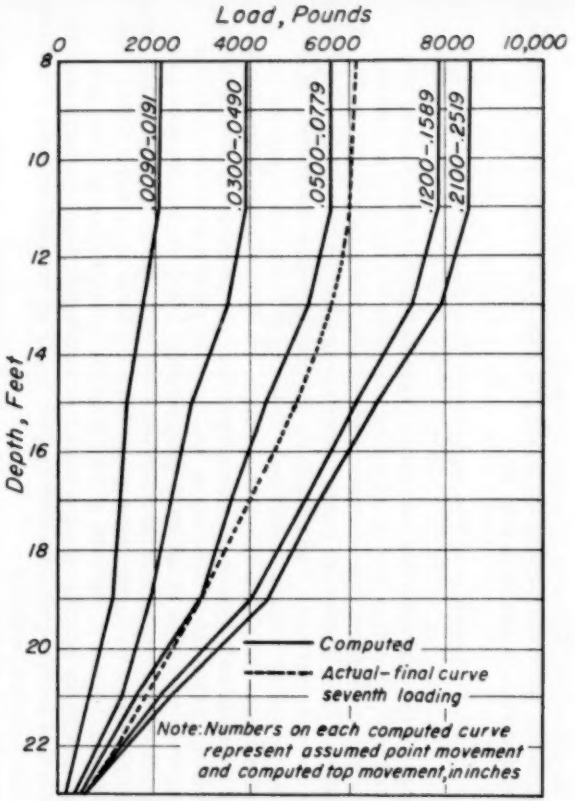

Fig. 19 COMPARISON OF COMPUTED AND ACTUAL LOAD DISTRIBUTION CURVES.

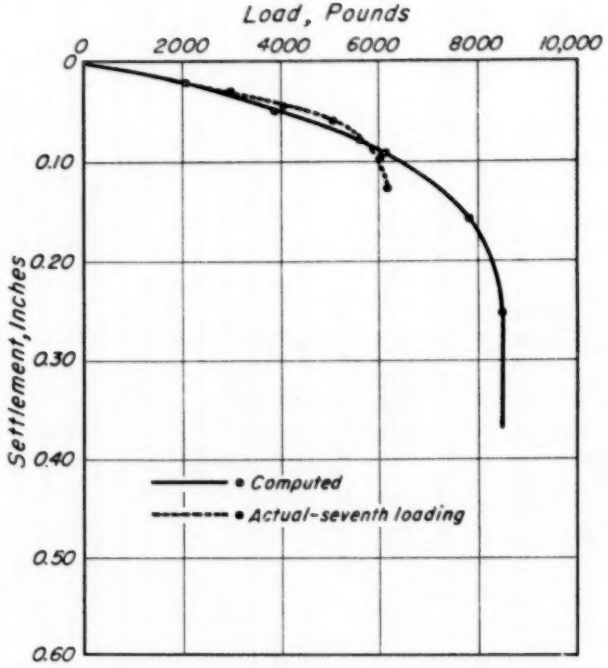

Fig. 20 COMPARISON OF COMPUTED AND ACTUAL LOAD *vs* SETTLEMENT CURVES.

modifications could then be made in the vane shear test data so that the load-settlement curves would agree. The modified vane shear test data could then be used to determine load distribution curves for other conditions of pile length and pile diameter.

The fact that the analysis does not take into account the deformation of the soil next to the pile wall caused by the non-uniform distribution of vertical load in the overlying soil would be expected to lead to computed settlements which are somewhat less than the actual settlements of the pile for any particular applied load; further investigation may reveal a simple method of taking this factor into account. Furthermore, the use of data obtained by vane shear tests on the undisturbed soil ignores the effect of pile driving on soil properties; it is possible that research will reveal a more suitable way of determining the soil properties to be used in the analysis.

Characteristics of Soil Adjacent to Driven Piles

In order to make a more accurate analysis of pile performance from soil tests, it would be necessary to be able to determine the characteristics of the soil adjacent to a driven pile. For this purpose it would be necessary to determine the properties of the partially remolded soil corresponding to points B and E on Figure 12 from the results of tests on soil samples obtained prior to pile driving. The properties of the undisturbed and completely remolded soil, corresponding to points A and C, could be established as previously described, and the slope of a line corresponding to B - E could be correctly obtained, but the positions of B and E would be indeterminate.

How much disturbance will occur due to the pile driving? In this investigation the tests show that in going from Point A to Point B the soil lost 67% of the strength it would have lost in being completely remolded. This does not mean that some other clay would lose the same proportion of its strength as a result of pile driving, even if the same type of pile were used.

The conservative assumption could be made that full remolding would occur. But it would still be necessary to determine the increase in strength of the soil due to reconsolidation. In these experiments the final strength of the soil next to the pile was about 60% more than the strength of the undisturbed soil, but there is no evidence to indicate that a different clay would show a similar increase in strength. Fully remolded soil attained a strength of 60% higher than the strength of the undisturbed soil when reconsolidated in the laboratory under a pressure of about 1 ton per sq ft (about one-half the total pressure which developed during driving), but this relationship may not be true for other piles.

Therefore, at this time a complete procedure for predicting the performance of friction piles from soil properties cannot be formulated and approximations must be made. It is believed, however, that the tests and analyses presented above do indicate a procedure for obtaining a reasonably accurate determination of pile performance, and that improved accuracy can be attained when basic work is done to determine the mechanics of the consolidation process around a pile driven into clay, to the end that peak pressures which are predicted can be translated into ultimate equilibrium pressures with accompanying consolidation and increase in shear strength of the clay.

SUMMARY

In the insensitive clay used in this investigation, the instrumented pile showed a marked increase in bearing capacity with time; the ultimate load

for the final load test, about 30 days after driving, was 5.4 times as great as the ultimate load measured several hours after driving. The increase in bearing capacity was attributed to an increase in the shear strength of the soil surrounding the pile.

The load distribution curves for the pile showed that most of the load was removed from the pile by shaft resistance, with only about 10% of any particular load reaching the pile tip. The increase in bearing capacity was reflected by an increase in the rate of load transfer, as determined by the slope of the load distribution curves; the increased rate of load transfer was exhibited by soil strata at all depths. The load distribution curves for all loadings showed a general increase in rate of load transfer with depth, with no load being removed by the soil near the ground surface and a maximum rate of about 400 lb per square foot being removed by soil at depths of 20 to 22 ft.

Strength-water content relationships were established for undisturbed soil and for fully remolded soil. Tests of soil samples taken next to the pile wall showed that the strength loss due to disturbance when the pile was driven was about 60% to 70% of that which the soil would have lost due to complete remolding. The clay next to the pile wall subsequently gained strength, and at the end of the test period it had a strength 60% higher than the strength of the undisturbed soil. This increase in soil strength appeared to parallel the decrease in excess hydrostatic pressure, and the data indicated that these phenomena are directly related.

The bearing capacity of the pile was not as great as would have been obtained if a shear resistance equal to the strength of the reconsolidated soil had been developed over the embedded area of the pile. This and related data led to the conclusion that the failure which occurred when the pile was overloaded occurred at the interface between pile and soil for the shallow depths, rather than in the soil.

A method was demonstrated for making a numerical solution of the differential equation governing the distribution of load from a friction pile to soil. From this procedure, the load vs. settlement relationship for a friction pile can be determined if the properties of the soil surrounding the pile are known. The method was applied to determine the performance of a test pile, using the stress-deformation characteristics of the undisturbed soil as determined by vane shear tests in the analysis. Results from the procedure were compared with experimental results, and fair agreement was obtained. It was suggested that better agreement would be obtained in a more homogeneous soil and if improved methods for determining soil properties could be developed. A procedure was also suggested for making the method useful in practice.

CONCLUSIONS

The conclusions listed below apply specifically to the investigation described in this paper; that is, to the study of a small-sized, displacement-type friction pile which was driven into a non-sensitive clay. The driving and testing procedures are, however, in many ways identical with practice, and it is believed that most of the conclusions will apply to other displacement-type friction piles having similar surface characteristics.

1) Even in an insensitive clay, the increase in bearing capacity of a displacement-type friction pile may be large, and the final bearing capacity may be as much as 5 times the initial bearing capacity.

2) The loss of strength of the soil around the pile was due to disturbance, caused by pile driving. As a result of this disturbance the soil lost about

70% of the strength it would have lost due to complete remolding. The shear strength of the disturbed and reconsolidated soil was 50% higher than the undisturbed shear strength.

3) For small values of time for all depths, and for all values of time for the shallow depths, the failure which occurred when the friction pile was over-loaded did not occur in the soil but at the interface between pile and soil.

4) The bearing capacity determined for a single friction pile by multiplying the area of the embedded pile by the soil shear strength obtained from unconfined compression tests of undisturbed samples, while being nearly equal to the true bearing capacity in some instances, must be considered an approximation.

5) Load vs. settlement curves and load distribution curves for a friction pile can be determined using a numerical procedure if the shear resistance vs. deformation relationship for the soil surrounding the pile can be determined.

6) The proposed method for determining the performance of a friction pile from soil tests is useful even in heterogeneous soil and using the shear resistance vs. deformation characteristics of the undisturbed soil as determined by vane shear tests, but better results could be obtained if shear resistance vs. deformation curves for reconsolidated soil adjacent to a driven pile could be determined.

ACKNOWLEDGMENT

The research was performed in the Engineering Materials Laboratory of the University of California and in the East Bay Yard of the San Francisco-Oakland Bay Bridge Railway. The permission of the Chief Engineer, San Francisco-Oakland Bay Bridge, of the California Division of Highways, to use the field test site is gratefully acknowledged. The authors also wish to thank the many members of the faculty and research staff of the Division of Civil Engineering and the Institute of Transportation and Traffic Engineering, University of California, who gave valuable advice and assistance in developing the instrumentation and accomplishing other phases of the work. Professors B. Bresler, D. Pirtz, R. Clough, and B. A. Vallerga gave valuable counsel regarding experimental procedures. Messrs. C. L. Monismith and F. N. Finn gave much help with the laboratory and field investigations. Messrs. R. Brock and L. Trescony gave assistance with the instrumentation, and the instruments and equipment were constructed by Messrs. E. L. Whittier and R. Lawrence. The assistance of Mr. G. Dierking who prepared the figures is also gratefully acknowledged.

REFERENCES

1. Housel, W. S., and Burkey, J. R., "Investigation to Determine the Driving Characteristics of Piles in Soft Clay," Proceedings, Second International Conference on Soil Mechanics, v. 5, 1948, pp. 146-154.

2. Cummings, A. E., Kerkhoff, G. O. and Peck, R. B., "Effect of Driving Piles into Soft Clay," Transactions, American Society of Civil Engineers, v. 115, 1950, pp. 275-350. See also discussion by P. C. Rutledge.

3. Rutledge, P. C., "Review of the Cooperative Triaxial Research Program" in Triaxial Shear Research and Pressure Distribution Studies on Soils; Soil Mechanics Fact-Finding Survey. U.S. Waterways Experiment Station, Vicksburg, Mississippi, April 1947. pp. 20-26 and 79-100.

4. Rutledge, P. C. "Strength of Natural Clays," paper presented at ASTM Meeting, Boston, Massachusetts, October 1948; Civil Engineering, November 1948, p. 23 (abstract).

5. Matlock, H., University of Texas. Derivation of differential equation given in letter to one of the authors, February, 1951.

PROCEEDINGS PAPERS

The technical papers published in the past year are identified by number below. Technical-division sponsorship is indicated by an abbreviation at the end of each Paper Number, the symbols referring to: Air Transport (AT), City Planning (CP), Construction (CO), Engineering Mechanics (EM), Highway (HW), Hydraulics (HY), Irrigation and Drainage (IR), Power (PO), Sanitary Engineering (SA), Soil Mechanics and Foundations (SM), Structural (ST), Surveying and Mapping (SU), and Waterways (WW) divisions. Papers sponsored by the Board of Direction are identified by the symbols (BD). For titles and order coupons, refer to the appropriate issue of "Civil Engineering" or write for a cumulative price list.

VOLUME 80 (1954)

DECEMBER: 558(ST), 559(ST), 560(ST), 561(ST), 562(ST), 563(ST)[c], 564(HY), 565(HY), 566(HY), 567(HY), 568(HY)[c], 569(SM), 570(SM), 571(SM), 572(SM)[c], 573(SM)[c], 574(SU), 575(SU), 576(SU), 577(SU), 578(HY), 579(ST), 580(SU), 581(SU), 582(BD).

VOLUME 81 (1955)

JANUARY: 583(ST), 584(ST), 585(ST), 586(ST), 587(ST), 588(ST), 589(ST)[c], 590(SA), 591(SA), 592(SA), 593(SA), 594(SA), 595(SA)[c], 596(HW), 597(HW), 598(HW)[c], 599(CP), 600(CP), 601(CP), 602(CP), 603(CP), 604(EM), 605(EM), 606(EM)[c], 607(EM).

FEBRUARY: 608(WW), 609(WW), 610(WW), 611(WW), 612(WW), 613(WW), 614(WW), 615(WW), 616(WW), 617(IR), 618(IR), 619(IR), 620(IR), 621(IR)[c], 622(IR), 623(IR), 624(HY)[c], 625(HY), 626(HY), 627(HY), 628(HY), 629(HY), 630(HY), 631(HY), 632(CO), 633(CO).

MARCH: 634(PO), 635(PO), 636(PO), 637(PO), 638(PO), 639(PO), 640(PO), 641(PO)[c], 642(SA), 643(SA), 644(SA), 645(SA), 646(SA), 647(SA)[c], 648(ST), 649(ST), 650(ST), 651(ST), 652(ST), 653(ST), 654(ST)[c], 655(SA), 656(SM)[c], 657(SM)[c], 658(SM)[c].

APRIL: 659(ST), 660(ST), 661(ST)[c], 662(ST), 663(ST), 664(ST)[c], 665(HY)[c], 666(HY), 667(HY), 668(HY), 669(HY), 670(EM), 671(EM), 672(EM), 673(EM), 674(EM), 675(EM), 676(EM), 677(EM), 678(HY).

MAY: 679(ST), 680(ST), 681(ST), 682(ST)[c], 683(ST), 684(ST), 685(SA), 686(SA), 687(SA), 688(SA), 689(SA)[c], 690(EM), 691(EM), 692(EM), 693(EM), 694(EM), 695(EM), 696(PO), 697(PO), 698(SA), 699(PO)[c], 700(PO), 701(ST)[c].

JUNE: 702(HW), 703(HW), 704(HW)[c], 705(IR), 706(IR), 707(IR), 708(IR), 709(HY)[c], 710(CP), 711(CP), 712(CP), 713(CP)[c], 714(HY), 715(HY), 716(HY), 717(HY), 718(SM)[c], 719(HY)[c], 720(AT), 721(AT), 722(SU), 723(WW), 724(WW), 725(WW), 726(WW)[c], 727(WW), 728(IR), 729(IR), 730(SU)[c], 731(SU).

JULY: 732(ST), 733(ST), 734(ST), 735(ST), 736(ST), 737(PO), 738(PO), 739(PO), 740(PO), 741(PO), 742(PO), 743(HY), 744(HY), 745(HY), 746(HY), 747(HY), 748(HY)[c], 749(SA), 750(SA), 751(SA), 752(SA)[c], 753(SM), 754(SM), 755(SM), 756(SM), 757(SM), 758(CO)[c], 759(SM)[c], 760(WW)[c].

AUGUST: 761(BD), 762(ST), 763(ST), 764(ST), 765(ST)[c], 766(CP), 767(CP), 768(CP), 769(CP), 770(CP), 771(EM), 772(EM), 773(SA), 774(EM), 775(EM), 776(EM)[c], 777(AT), 778(AT), 779(SA), 780(SA), 781(SA), 782(SA)[c], 783(HW), 784(HW), 785(CP), 786(ST).

SEPTEMBER: 787(PO), 788(IR), 789(HY), 790(HY), 791(HY), 792(HY), 793(HY), 794(HY)[c], 795(EM), 796(EM), 797(EM), 798(EM), 799(EM)[c], 800(WW), 801(WW), 802(WW), 803(WW), 804(WW), 805(WW), 806(HY), 807(PO)[c], 808(IR)[c].

OCTOBER: 809(ST), 810(HW)[c], 811(ST), 812(ST)[c], 813(ST)[c], 814(EM), 815(EM), 816(EM), 817(EM), 818(EM), 819(EM)[c], 820(SA), 821(SA), 822(SA)[c], 823(HW), 824(HW).

NOVEMBER: 825(ST), 826(HY), 827(ST), 828(ST), 829(ST), 830(ST), 831(ST)[c], 832(CP), 833(CP), 834(CP), 835(CP)[c], 836(HY), 837(HY), 838(HY), 839(HY), 840(HY), 841(HY)[c].

DECEMBER: 842(SM), 843(SM)[c], 844(SU), 845(SU)[c], 846(SA), 847(SA), 848(SA)[c], 849(ST)[c], 850(ST), 851(ST), 852(ST), 853(ST), 854(CO), 855(CO), 856(CO)[c], 857(SU), 858(BD), 859(BD), 860(BD).

c. Discussion of several papers, grouped by Divisions.

AMERICAN SOCIETY OF CIVIL ENGINEERS

OFFICERS FOR 1956

PRESIDENT

ENOCH RAY NEEDLES

VICE-PRESIDENTS

Term expires October, 1956:
FRANK L. WEAVER
LOUIS R. HOWSON

Term expires October, 1957:
FRANK A. MARSTON
GLENN W. HOLCOMB

DIRECTORS

Term expires October, 1956:
WILLIAM S. LaLONDE, JR.
OLIVER W. HARTWELL
THOMAS C. SHEDD
SAMUEL B. MORRIS
ERNEST W. CARLTON
RAYMOND F. DAWSON

Term expires October, 1957:
JEWELL M. GARRELTS
FREDERICK H. PAULSON
GEORGE S. RICHARDSON
DON M. CORBETT
GRAHAM P. WILLOUGHBY
LAWRENCE A. ELSENER

Term expires October, 1958
JOHN P. RILEY
CAREY H. BROWN
MASON C. PRICHARD
ROBERT H. SHERLOCK
R. ROBINSON ROWE
LOUIS E. RYDELL
CLARENCE L. ECKEL

PAST-PRESIDENTS

Members of the Board

DANIEL V. TERRELL
WILLIAM R. GLIDDEN

EXECUTIVE SECRETARY
WILLIAM H. WISELY

TREASURER
CHARLES E. TROUT

ASSISTANT SECRETARY
E. L. CHANDLER

ASSISTANT TREASURER
CARLTON S. PROCTOR

PROCEEDINGS OF THE SOCIETY

HAROLD T. LARSEN
Manager of Technical Publications

DEFOREST A. MATTESON, JR.
Editor of Technical Publications

PAUL A. PARISI
Assoc. Editor of Technical Publications

COMMITTEE ON PUBLICATIONS

SAMUEL B. MORRIS, *Chairman*

JEWELL M. GARRELTS, *Vice-Chairman*

ERNEST W. CARLTON
MASON C. PRICHARD
R. ROBINSON ROWE
LOUIS E. RYDELL